Tetracycline-Tet Repressor Binding Specificity: Insights from Experiments and Simulations

Alexey Aleksandrov,[†] Linda Schuldt,[‡] Winfried Hinrichs,[‡*] and Thomas Simonson[†*]
[†]Laboratoire de Biochimie, Department of Biology, Ecole Polytechnique, Centre National de la Recherche Scientifique UMR 7654, Palaiseau, France; and [‡]Institute for Biochemistry, Department of Molecular Structural Biology, University of Greifswald, Greifswald, Germany

ABSTRACT Tetracycline (Tc) antibiotics have been put to new uses in the construction of artificial gene regulation systems, where they bind to the Tet repressor protein (TetR) and modulate its affinity for DNA. Many Tc variants have been produced, both to overcome bacterial resistance and to achieve a broad range of binding strengths. To better understand TetR-Tc binding, we investigate a library of 16 tetracyclines, using fluorescence experiments and molecular dynamics free energy simulations (MDFE). The relative TetR binding free energies are computed by reversibly transforming one Tc variant into another during the simulation, with no adjustable parameters. The chemical variations involve polar and nonpolar substitutions along one entire edge of the elongated Tc structure, which provides many of the protein-ligand contacts. The binding constants span five orders of magnitude. The simulations reproduce the experimental binding free energies, when available, within the uncertainty of either method ($\pm$0.5 kcal/mol), and reveal many additional details. Contributions of individual Tc substituents are evaluated, along with their additivity and transferability among different positions on the Tc scaffold; differences between D- and B-class repressors are quantified. With increasing computer power, the MDFE approach provides an attractive complement to experiment and should play an increasing role in the understanding and engineering of protein-ligand recognition.

INTRODUCTION

Tetracycline (Tc) is an important antibiotic, which binds to the bacterial ribosome and blocks protein synthesis (1–3). Although >1000 Tc variants have been synthesized, only a handful can be used as broad-spectrum antibiotics for humans and livestock. Widespread use has led to several resistance mechanisms, including mutations in the bacterial rRNA and export of Tc from the cell (1,4,5). It is thus important to develop new Tcs that can evade resistance while effectively inhibiting protein synthesis. Tc export from the bacterial cell is controlled by the Tet Repressor protein (TetR). In the absence of Tc, TetR binds to the bacterial DNA as a homodimer and represses the resistance genes. When Tc is present, it binds to TetR as a $[Tc\ Mg]^+$ complex with a nanomolar dissociation constant, inducing conformational changes that reduce the binding constant of TetR and DNA by 6–10 orders of magnitude (6–8). TetR dissociates from the DNA, triggering the expression of a membrane export protein, TetA (1).

Today, the TetR-Tc system is of general interest because of widespread application in molecular and cell biology as a sensitive switch for target gene regulation (9–12). Both the protein and the ligand have been engineered to give modified gene regulation systems. Thus, directed evolution has yielded mutant TetRs that are induced by specific Tcs, including nonantibiotic variants (13). Mutants have been obtained that have an inverse behavior: binding a Tc variant enhances the DNA binding affinity (14,15). A small peptide agonist was obtained recently, which can induce TetR as efficiently as Tc (16,17). Functional TetRs have been constructed where the two subunits are fused into a single chain, including one variant that has different affinities for specific Tcs in its two binding pockets (18).

The main features of TetR-Tc recognition have been revealed by crystallography (7,8,19) and biochemical measurements (13,20–23). Crystal structures are available for TetR in its induced state, in complex with several Tc variants (5,19,24–26). The structure of noninduced TetR is known, bound either to the operator DNA (7) or as apo-TetR (27). Also available is a half-induced structure, with $[Tc\ Mg]^+$ bound to just one of the two monomers, which adopts the induced conformation, whereas the other monomer is in the noninduced conformation, with bound Tc but no associated Mg^{2+} (28).

Despite the wealth of data, many important details are not revealed by crystallography. Thus, Tc has two main tautomers, which are hard to distinguish crystallographically, but have very different charge distributions. Several side chains around the binding pocket can adopt different orientations and protonation states that are hard to distinguish. An earlier study used special x-ray refinement methods and free energy simulations to explore these degrees of freedom in the bound and unbound states (29), and showed that they are preorganized for Tc-TetR binding.

Here, we investigate the sources of TetR-Tc binding specificity, by comparing the TetR binding affinities of Tc and 15 variants. Again, the binding preferences are the result of a competition between many different effects, including

Submitted July 8, 2009, and accepted for publication August 31, 2009.

*Correspondence: thomas.simonson@polytechnique.fr or winfried.hinrichs@uni-greifswald.de

Linda Schuldt's present address is EMBL Hamburg, c/o DESY, Notkestrasse 85, D-22603 Hamburg, Germany.

Editor: Axel T. Brunger.

0006-3495/09/11/2829/10 $2.00

doi: 10.1016/j.bpj.2009.08.050

desolvation of protein and ligand, plasticity of the binding site, and direct protein-ligand contacts. To elucidate these effects, we use a combination of thermodynamic measurements and molecular dynamics (MD) simulations. We compare Tc variants by alchemically transforming one into the other, during a series of MD simulations. We also consider several point mutants of TetR. The transformation of ligand or protein is done reversibly, both for the TetR-ligand complex and for the isolated ligand or protein in solution, so that a binding free energy difference is obtained (30). We refer to this technique as molecular dynamics free energy simulations (MDFE) (30–34). Thanks to a recently developed force-field model for tetracyclines (35,36), the simulations reproduce experimental binding free energy differences to within the experimental error, ± 0.5 kcal/mol. Indeed, a second goal of this work is to illustrate the maturity of free energy simulations for molecular recognition (33,34).

An approach combining experiments and simulations is especially valuable to elucidate the fine details of binding specificity. With MDFE, atomistic structural information and thermodynamic information are derived from the same MD simulations. We can examine the contributions of individual chemical groups to binding (such as methyl or hydroxyl groups) and the transferability of such contributions from one position to another on the Tc scaffold. We also consider the additivity of effects arising when two groups are added or removed at different positions. Group effects are further characterized by their individual contributions to the free energy changes, usually referred to as free energy components (37–39). We consider solvent contributions, as well as subtle differences between the D- and B-class Tet Repressors (TetR(D) and TetR(B), respectively).

Our analysis also illustrates the modular structure of tetracyclines. Indeed, Tcs are elongated, fused-ring molecules, with an upper and a lower edge (Fig. 1). The lower edge chelates a metal ion and presents it to the TetR protein (24,40). The Tc and TetR modifications considered here are mostly located on the opposite, upper edge. They illustrate its role as a specificity edge, which tunes the strength of TetR binding. This analysis should aid efforts to design further variants of Tc and of the Tet Repressor, and to engineer improved and more-diverse systems for artificial gene regulation.

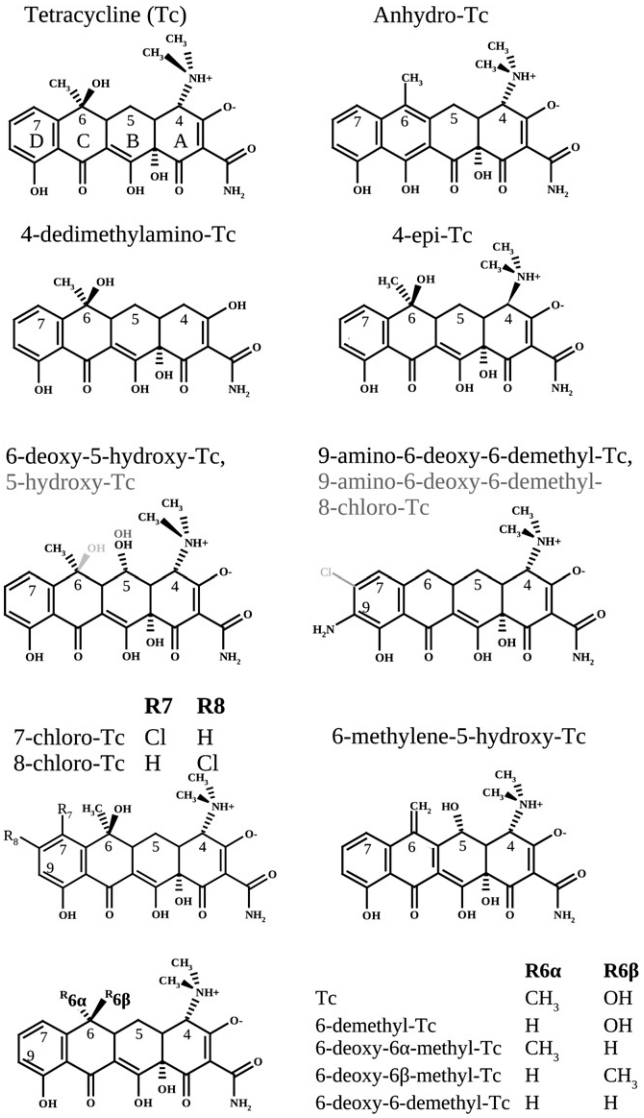

FIGURE 1 Tetracycline (Tc) and the analogs studied in this work.

METHODS

Binding measurements

TetR(D) was expressed and purified as described previously (27). Tetracyclines were dissolved in degassed H_2O and used for a maximum of 24 h. No degradation was detected during this time by measuring UV spectra and binding constants to TetR(D). TetR(D)/[Tc Mg]$^+$ binding constants were obtained by fluorescence titration at 20°C (Fluorimeter LS50B, PerkinElmer, Boston, MA). The same buffer (5 mM $MgCl_2$, 50 mM Tris/HCl pH 8.0, 150 mM NaCl) was used for all titrations. Protein solution (0.05–1 μM) in buffer with sufficient Mg^{2+}-concentration to ensure complete [Tc Mg]$^+$ formation was titrated with equal amounts of tetracycline stock solutions (1.5–4 μM) (compare (41)). Titration was performed at optimized wavelengths from excitation and emission spectra of the TetR(D)/[Mg Tc]$^+$ complexes. Recently, we described the method in detail (see method *A* in (26)).

Molecular dynamics simulations

The crystal structure of the class D Tet Repressor (TetR(D)) was taken from the Protein Data Bank (PDB), entry 2TRT (with bound Tc) (19). The simulations included protein residues within a 24 Å sphere, centered on the Tc binding site. In addition to crystal waters, a 24 Å sphere of water was overlaid, and waters that overlapped protein, crystal waters, Tc, or Mg^{2+}, were removed. Protein atoms between 20 Å and 24 Å from the sphere's center were harmonically restrained to their experimental positions. Simulations were done with the SSBP solvent model (42,43), which treats the region outside the 24 Å sphere as a uniform dielectric continuum, with a dielectric constant of 80. This is reasonable, since most of the outer region is water. Newtonian dynamics were used for the innermost region, within 20 Å of the sphere's center; Langevin dynamics were used for the outer part of the sphere, with a 292 K bath. The CHARMM22 force field was used for the protein (44) and the TIP3P model for water (45). Tetracyclines were described with the force field developed previously (35,36). Electrostatic

interactions were computed without any cutoff, using a multipole approximation for distant groups (46). Calculations were done with the CHARMM program (47,48).

Alchemical MD free energy simulations (MDFE)

To compare TetR binding by Tc and an analog, Tc′, we use a standard thermodynamic cycle (33,49). The two vertical legs represent Tc (respectively, Tc′) binding to TetR. The MDFE method follows the horizontal legs, and reversibly transforms Tc into Tc′ during a series of MD simulations. For the lower leg, we simulate $[\mathrm{Tc\ Mg}]^+$ in the center of a 24 Å radius water sphere, surrounded by a dielectric continuum representing bulk solvent (42). For the upper leg, we simulate a portion of the $[\mathrm{Tc\ Mg}]^+$-TetR complex, solvated by the same 24 Å water sphere and embedded in the same dielectric continuum. Portions of TetR outside the 24 Å sphere are expected to contribute very little to the binding free energy difference (43). In each simulation system, the energy function can be expressed as a linear combinations of Tc and Tc′ terms,

$$U(\lambda) = U_0 + (1-\lambda)U(\mathrm{Tc}) + \lambda U(\mathrm{Tc}'), \qquad (1)$$

where λ is a coupling parameter and U_0 represents interactions between parts of the system other than Tc. In our implementation, which uses the CHARMM program, this energy form is obtained by explicitly modifying selected force-field parameters at each λ-value and by manually excluding unwanted interatomic interactions (through the CHARMM exclusion statement). The free energy derivative with respect to λ has the form

$$\frac{\partial G}{\partial \lambda}(\lambda) = \left\langle U(\mathrm{Tc}') - U(\mathrm{Tc}) \right\rangle_\lambda, \qquad (2)$$

where the brackets indicate an average over an MD trajectory with the energy function $U(\lambda)$ (33,49). We gradually mutated Tc into Tc′ by changing λ from zero to one. The successive values of λ were 0.001, 0.01, 0.05, 0.1, 0.2, 0.4, 0.6, 0.8, 0.9, 0.95, 0.99, and 0.999. The free energy derivatives were computed at each λ-value from a 100-ps MD simulation, or window; the last 80 ps of each window were used for averaging. A complete mutation run thus corresponded to 12 windows and 1.2 ns of simulation. Three runs were performed in each direction (Tc into Tc′ and the reverse), starting from equilibrated structures separated by 1 ns of dynamics. The derivatives are used to obtain ΔG, using trapezoidal integration, except for van der Waals contributions close to the endpoints of the mutation (λ = 0.0–0.001 and 0.999–1.0). For these endpoint contributions, analytical integration was used (50). The total CPU time for a single MDFE run was ~48 h on a recent, 64-bit, desktop machine (3 GHz Intel processor with 4 Mbytes of cache, using a single core).

Accurate uncertainty estimation with MDFE is difficult and expensive (51–53). A widely-used approach is to perform multiple runs and measure the dispersion between runs. Although this seems plausible, it neglects some forms of systematic error, and can actually lead to an overestimated uncertainty. In particular, it is well known that runs performed in opposite directions (forward and backward transformations; λ increasing or decreasing) exhibit systematic hysteresis effects (54–56). Thus, we use an error estimator that considers pairs of runs, one in each direction, forming a forward/backward pair (40,57,58). In previous work, these forward/backward averages were much more reproducible than the individual values. The uncertainty is taken to be their standard deviation (usually obtained from three forward/backward pairs, totaling 7.2 ns). In a few cases, we considered only half of each window, yielding artificially shortened runs; the effect on the overall ΔG values was comparable to our uncertainty estimates, indicating that our run lengths are reasonable. (For a more detailed discussion of convergence and some examples, see the Supplementary Material in (40).)

Almost all of the tetracycline variants were produced by directly modifying Tc. For the largest ligand variations, however, a two-step transformation was used. For example, 9-amino-6-deoxy-6-demethyl-Tc was obtained from 6-deoxy-6-demethyl-Tc, and 9-amino-8-chloro–6-deoxy-6-demethyl-Tc was obtained from 9-amino-6-deoxy-6-demethyl-Tc. In a few cases, multiple pathways were compared. For example, 6-deoxy-6β-methyl-Tc was obtained in three different ways: either from 6-deoxy-6-demethyl-Tc, from 6-deoxy-6α-methyl-Tc, or from 6-deoxy-5-hydroxy-Tc; the three free energy estimates (−2.3, −2.5, −2.6 kcal/mol) agree within the estimated statistical uncertainty (±0.2 kcal/mol for this ligand; Table 1). In other cases where two or more pathways were compared, the variations in

TABLE 1 Tetracyclines binding to TetR: experiment versus simulations

			$\Delta\Delta G_{\mathrm{MDFE}}$	$\Delta\Delta G_{\mathrm{exptl}}$	
Tc variant	ΔG_{prot}[†]	ΔG_{sol}[†]	TetR(D)	TetR(D)[‡]	TetR(B)[§]
4-Dedimethylamino	3.4(0.6)	−1.2(0.1)	4.6(0.7)	—	4.8(0.6)
4-Epi	2.7(0.4)	−0.1(0.1)	2.8(0.4)	—	3.4(0.4)
5-Hydroxy	−0.6(0.3)	−1.0(0.3)	0.4(0.4)	0.0(0.4)	0.1(0.5)
6-Deoxy-5-hydroxy	−1.1(0.9)	1.0(0.3)	−2.1(0.9)	−1.5(0.5)	−1.2(0.4
6-Methylene-5-hydroxy	−1.3(0.9)	0.1(0.3)	−1.4(0.9)[¶]	—	−1.2(0.3)
6-Deoxy-6α-methyl	2.8(0.2)	5.1(0.1)	−2.4(0.2)	—	—
6-Deoxy-6β-methyl	−1.4(0.3)	−0.2(0.2)	−1.3(0.4)[¶]	—	0.4(0.5)
6-Demethyl	2.2(0.2)	1.5(0.2)	0.7(0.2)	—	1.8(0.6)
6-Deoxy-6-demethyl	−0.9(0.2)	0.8(0.1)	−1.8(0.2)	−1.5(0.5)	−0.5(0.6)
Anhydro-Tc	−4.7(0.8)	−1.7(0.3)	−2.9(0.9)	−2.4(0.4)	−2.1(0.4)
7-Chloro	2.2(0.1)	3.0(0.1)	−0.8(0.1)	−0.5(0.5)	−0.6(0.6)
8-Chloro	0.9(0.4)	1.7(0.1)	−0.8(0.4)	—	—
8-Methyl	−1.4(0.3)	−0.8(0.1)	−0.6(0.3)	—	—
9-Amino-6-deoxy-6-demethyl	−3.6(0.3)	−4.0(0.2)	0.4(0.4)[¶]	—	0.7(0.7)
9-Amino-8-chloro-6-deoxy-6-demethyl	−2.7(0.3)	−2.0(0.2)	−0.7(0.4)[¶]	—	−0.5(0.5)

Relative binding free energies (kcal/mol), with Tc as a reference. The Tc-TetR(D) binding free energy is −12.4 kcal/mol (this work). Experimental values are from Lederer et al. (41) or this work.

[†]Columns 2–3 are the free energy to reversibly modify Tc, either in complex with TetR(D) (ΔG_{prot}) or in solution (ΔG_{sol}). For clarity, the free energy to modify Tc in vacuum has been subtracted in each case (see main text). The binding free energy change can be written as $\Delta\Delta G = \Delta G_{\mathrm{prot}} - \Delta G_{\mathrm{sol}}$. A negative $\Delta\Delta G$ means the variant binds more strongly than Tc. Experimental and MDFE error bars are in parentheses.

[‡](TetR(D)).

[§](TetR(B)).

[¶]Estimated using two sequential transformations of the ligand (see Methods).

the free energies were consistent with the estimated uncertainties (e.g., for 6-deoxy-6α-methyl-Tc; data not shown).

Free energy component analysis

The contribution of an individual atom i (that is not part of the ligand) to the free energy derivative can be calculated by writing the energy function as

$$U(\lambda) = \sum_{i} U_{i0}(\lambda) + \sum_{i<j} U_{ij} + U_{lig}(\lambda), \quad (3)$$

where $U_{i0}(\lambda)$ contains the interaction energy terms between atom i and the ligand, U_{ij} represents the interactions between i and atoms not in the ligand, and U_{lig} represents interactions within the ligand. Only the terms U_{i0} and U_{lig} depend on λ. Thus, atom i contributes a term

$$\partial G_i/\partial\lambda = \langle \partial U_{i0}/\partial\lambda \rangle_\lambda \quad (4)$$

to the free energy derivative. The numerical integration is linear, so the numerical integral is equal to the sum of the integrals of the individual $\partial G_i/\partial\lambda$. Summing over groups of atoms or residues, one obtains the free energy contribution directly associated with each group. In the same way, one can obtain the free energy contribution associated with specific energy terms, e.g., the Coulomb or van der Waals terms in the energy function, either for a specific group or for the whole system (except the ligand itself). We refer to the component arising from the Coulomb term as the electrostatic component. Free energy components should be interpreted with care, since the values obtained depend on details of the calculation, such as the precise pathway employed (38,39). The alchemical pathway used here, transforming one tetracycline into another, is thought to provide the most useful components (38,39).

RESULTS

MDFE yields binding free energies with chemical accuracy

We begin by comparing experimental and computed binding free energy differences, to establish the accuracy of the simulations. Indeed, Table 1 reports relative binding free energies for 16 tetracyclines. The experimental TetR(D) binding free energy for Tc, taken as a reference, is -12.4 ± 0.1 kcal/mol (this work). The Tc modifications involve positions 4–9 on the Tc scaffold (Figs. 1 and 2). For six of the Tcs, binding to the D-class repressor, TetR(D), was measured in this work, using fluorescence titration (see Methods). For the other 10 Tcs in Table 1, either the molecule was not readily available or its fluorescence properties were not suitable. For 13 of the Tcs, the experimental binding affinity for the homologous repressor, TetR(B), is known (59) (last column in Table 1). MDFE results are given for each Tc variant, binding to TetR(D). We established earlier that Tc prefers its zwitterionic tautomer (N_4 protonated, O_3 deprotonated; see Fig. 1), both in solution and in complex with TetR (29,35). We assume the variants considered here are also zwitterionic, since they have the same A ring as Tc (for Tc ring labels, see Fig. 1). This assumption is supported by the good agreement between experiment and simulations.

Fig. 3 plots the computed versus the experimental binding free energies. For the various Tcs binding to TetR(D), the agreement is excellent, with a root mean-square (RMS) deviation of just 0.44 kcal/mol. This deviation is averaged over five binding free energy values; it is comparable to the statistical uncertainty of experiment and simulations, ± 0.5 kcal/mol on average. In four cases, the experimental binding is stronger than the computed binding; however, the differences remain small and within the statistical uncertainty of the method. Note that the Tc-TetR(D) affinities were measured after the simulations were done. Thus, MDFE predicts the Tc-TetR(D) binding free energies with a high accuracy and precision.

The inset in Fig. 3 shows all 16 ligands, taken from their respective MDFE simulations. The 16 protein backbone structures were superimposed, and the resulting ligand conformations collected. Only the main, four-ring scaffold of each ligand is shown, for clarity. We see that the ligand variations produce only small shifts in the ligand position within its binding pocket. For two Tc variants, 6-deoxy-5-hydroxy-Tc and 7-chloro-Tc, TetR(D)-ligand x-ray structures are available (PDB entries 2O7O and 2FJ1, respectively) (24,26), to which the MDFE structures can be compared. Comparing PDB No. 2O7O to the structures from the end of the Tc → 6-deoxy-5-hydroxy-Tc transformation, for example, gives an overall RMS coordinate deviation of 0.89 Å for protein backbone atoms (excluding those that are restrained during the simulation) and 0.59 Å for the ligand

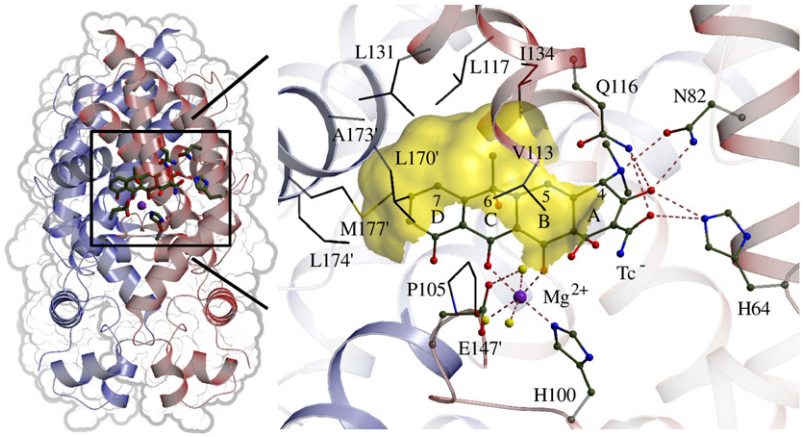

FIGURE 2 Overview of the Tc-TetR complex (*left*) and closeup of the binding site (*right*). The N-terminal, DNA binding domains are at the bottom of the left-hand view. Secondary structure elements belonging to monomer 1 (respectively, 2) are red (*blue*). A magnesium ion and associated waters are shown as spheres. Important polar residues are shown in ball-and-stick representation. Hydrophobic residues are shown as lines. Primed residues belong to monomer 2. The surface of the hydrophobic pocket created by these residues is shown in yellow. The Tc rings are labeled; selected atoms are numbered (as in text).

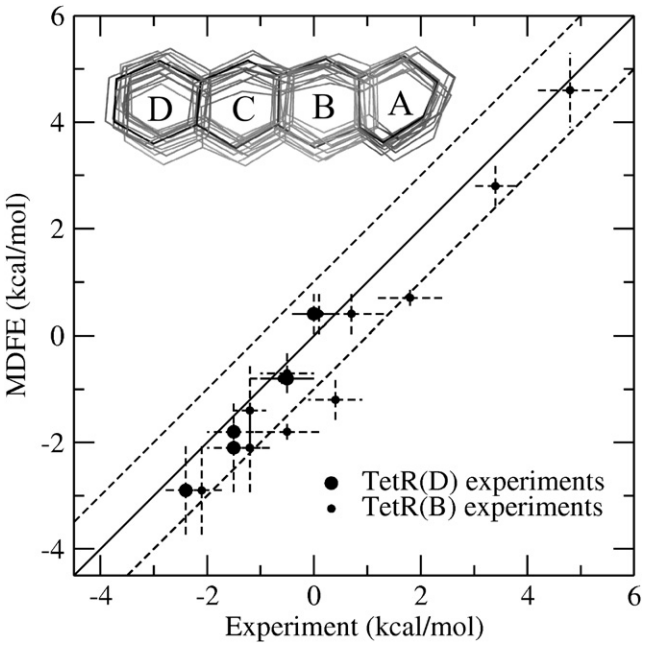

FIGURE 3 Experimental and computed binding free energies for 16 tetracycline variants are compared. Results are given relative to Tc. Experimental and computed error bars are shown. The solid line corresponds to a perfect match between experimental and computed values; dashed lines are 1 kcal/mol above/below. All the MDFE simulations employ the D-class repressor. The experimental data correspond to either TetR(D) (*large dots*) or the homologous TetR(B). (*Inset*) All 16 ligands, superimposed based on the protein structure. For clarity, only the main, fused-ring scaffold is shown; Tc is black, the other ligands are gray.

(deviations averaged over the last 200 ps of simulation). For the Tc → 7-chloro-Tc case, the backbone RMS deviation between the MDFE structure and the 2FJ1 x-ray structure is 1.21 Å (0.87 Å for the ligand). These deviations are small, and typical of current MD simulations; they are comparable to those observed for a recent simulation of the Tc-TetR(D) complex: 0.75 Å for the backbone and 1.05 Å for atoms close to the Tc ligand (29).

For seven Tcs, experimental data are available for TetR(B) binding, but not for TetR(D), so that a precise comparison to MDFE is not possible. In the five cases where the experimental TetR(B) and TetR(D) binding free energies are both available, they have an RMS deviation of 0.49 kcal/mol. Four of the five deviations are very small (0.3 kcal/mol or less), whereas 6-deoxy-6-demethyl has a 1 kcal/mol deviation. Comparing the MDFE results for TetR(D) to the same five experimental TetR(B) results gives a slightly higher RMS deviation of 0.69 kcal/mol. In three cases (including 6-deoxy-6-demethyl-Tc), the difference between experiment (TetR(B)) and MDFE (TetR(D)) is >0.8 kcal/mol. For 6-deoxy-6-demethyl-Tc, MDFE and experiment agree closely. For aTc and 6-deoxy-5-hydroxy-Tc, the MDFE/TetR(B) differences are 0.8 and 0.9 kcal/mol, respectively, whereas the experimental D/B differences are 0.3 kcal/mol; i.e., smaller but with the same sign as the MDFE result. For aTc binding to TetR(B), preliminary experimental results suggest that the published affinity (41) may not be fully reliable (W. Hinrichs, unpublished data). In any case, the experimental/MDFE differences for these two ligands are still within the statistical uncertainty of the two methods. Overall, MDFE can be compared qualitatively to the TetR(B) experiments, and can be used to predict the larger TetR(D)/TetR(B) differences (which are considered in detail further on).

Hydroxyl editing at positions 5 and 6

In this and the next two sections, we consider specific Tc variations and their effect on TetR binding. The ligands in Table 1 provide opportunities to sample the effect of hydroxyl groups in different contexts, at positions 5 and especially 6. Table 1 reports the binding free energy changes, $\Delta\Delta G$, along with the individual free energy changes in the protein complex and in solution, ΔG_{prot} and ΔG_{solv}. The free energy change for the transformation in vacuum has been subtracted, effectively removing the contribution of intraligand interactions, and allowing the free energy changes to be interpreted in terms of protein-ligand and solvent-ligand interactions. Below, we make use of a further decomposition of the free energy changes into components (see Methods). These correspond to contributions from either the van der Waals or the Coulomb (or electrostatic) term in the energy function, which arise either from the entire protein or a specific amino acid.

Introducing a hydroxyl at position 5 hardly changes the binding affinity, either for TetR(B) or TetR(D) (see 5-hydroxy-Tc in Table 1). In the protein, the 5-hydroxyl makes a hydrogen bond to the Gln^{116} side chain, which also interacts with the 2,3-ketone-enolate group of Tc (Fig. 2). This hydrogen bond replaces a hydrogen bond to water, and balances the 5-hydroxyl desolvation penalty.

In contrast, a hydroxyl at position 6 lacks a hydrogen-bonding partner in the protein; the shortest distance to a polar TetR group is to the Gln^{116} side chain, 4.9 Å away. The hydrophobic residues Pro^{105} and Val^{113} are closer by (Fig. 4 *A*). Thus, the binding free energy of 6-deoxy-6α-methyl-Tc is 2.4 ± 0.2 kcal/mol higher than that of Tc. This is consistent with estimates of free energy contributions of nonionic hydrogen bonds (60–62). Intuitively, it represents the penalty to remove the polar, hydroxyl group from water. Comparing the free energy changes in the protein and in solution, ΔG_{prot} and ΔG_{solv}, we see that the largest free energy component is a large, positive, electrostatic contribution to ΔG_{solv}: +5.1 kcal/mol, opposing removal of the hydroxyl from solvent (Table 1). The electrostatic component in the protein is also positive but much smaller: +2.8 kcal/mol. Note that the nearby Pro^{105} and Val^{113} have negligible components (0.1 kcal/mol each). Thus, the binding free energy change can indeed be quantitatively ascribed to lost electrostatic interactions in the unbound state.

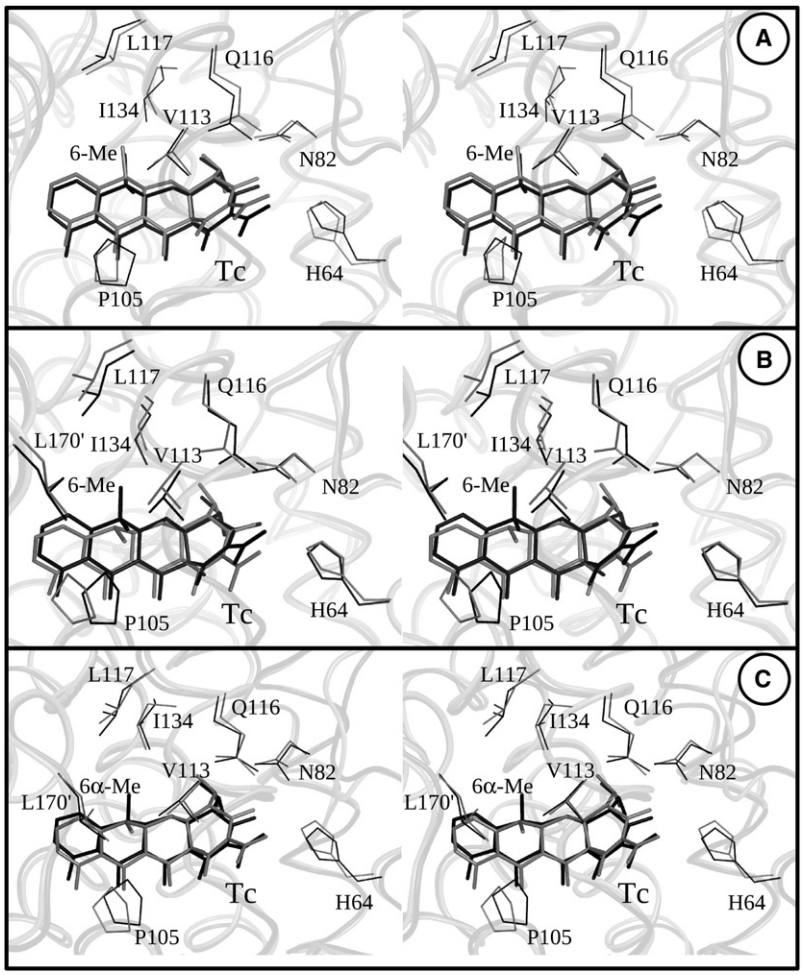

FIGURE 4 MD structures of selected complexes (divergent stereo). (*A*) Tc and 6-deoxy-Tc complexes. The Tc complex is black (ligand and protein side chains); the 6-deoxy-Tc complex is gray. The ligands and nearby hydrophobic residues are shown as sticks, the protein backbones as ribbons. The Tc 6-methyl is labeled. (*B*) Tc and 6-demethyl-Tc complexes; same representation. (*C*) 6α-methyl-6-deoxy-Tc and 6β-methyl-6-deoxy-Tc complexes. The 6α-methyl-6-deoxy-Tc complex is black; the 6β-methyl-6-deoxy-Tc complex is gray.

Six-deoxy-6α-methyl-Tc is predicted to be one of the strongest-binding Tc variants (Table 1). No experimental binding free energy is available, but we may compare the hydroxyl effect in other contexts. The difference between 6-demethyl-Tc and 6-demethyl-6-deoxy-Tc is 2.5 kcal/mol (MDFE, TetR(D)) or 2.3 kcal/mol (experiment, TetR(B)). Thus, the hydroxyl contribution is transferable from Tc to 6-demethyl-Tc. Not only the total effect, but the separate van der Waals and electrostatic contributions to ΔG_{prot} and ΔG_{solv}, are very similar (not shown). Comparing 5-hydroxy-Tc and 6-deoxy-5-hydroxy-Tc gives a somewhat lower difference of 1.5 kcal/mol for TetR(D) binding (2.5 kcal/mol with MDFE), or 1.3 kcal/mol for TetR(B). Finally, with aTc, we have removed the 6-hydroxyl, but also the 6-hydrogen, leading to a planar C ring. The binding free energy gain is 2.4 $\pm$ 0.4 kcal/mol (2.9 $\pm$ 0.9 kcal/mol with MDFE). This is consistent with the 6-hydroxyl effect in other contexts, and supports the idea that the binding variations are governed by desolvation.

Hydrophobic groups at positions 6–8 increase Tc binding

Our ligand set includes two pairs that differ by a 6-methyl group (in the α-orientation): Tc/6-demethyl-Tc and 6-deoxy-6α-methyl-Tc/6-deoxy-6-demethyl-Tc. The two binding free energy differences are 0.7 and 0.6 kcal/mol, favoring the methylated form. The latter value is an average over two sets of MDFE simulations that follow two distinct pathways: a direct transformation and an indirect transformation, via Tc; the two simulations yield 0.5 and 0.7 kcal/mol, respectively, in good mutual agreement. The affinity decrease upon demethylation can be attributed to the favorable desolvation of the methyl when it is present, and its burial in a hydrophobic pocket in the complex (Fig. 2 and Fig. 4 *B*). It represents an example of solvent interactions driving binding, as well as another example of transferability of a substituent effect from one context (Tc) to another (6-deoxy-Tc). If the 6-methyl is replaced by a methylene, binding is reduced by a similar amount, 0.7 kcal/mol (compare 6-deoxy-5-hydroxy and 6-methylene-5-hydroxy). The methylene is similar to the 6-methyl in size and polarity, but it is in plane with the C ring and has a different orientation with respect to the protein environment. Finally, if the 6-methyl is moved from the 6α orientation (as in Tc) to the 6β orientation, the effect on binding is no longer favorable, because of steric conflict between the methyl and Val^{113} (Fig. 4 *C*). Indeed, for this transformation, the van

der Waals component is precisely equal to the total binding free energy change, 1.3 ± 0.5 kcal/mol; the electrostatic component is zero.

Six-demethylation is the only ligand change that has a substantially different effect in TetR(D) and TetR(B): see 6-demethyl-Tc and 6-deoxy-6-demethyl-Tc in Table 1. For these two Tc variants, as well as 6-deoxy-6βmethyl-Tc, the TetR(D)/TetR(B) difference is ~+1 kcal/mol, indicating that the 6-methyl makes superior interactions with TetR(B) (or the 6-demethyl variants make inferior interactions). In TetR(D), the 6-methyl contacts Val^{113}, Leu^{117}, Leu^{131}, and Ile^{134}, with methyl-methyl distances of 4.5, 4.1, 5.3, and 4.1 Å, respectively (Fig. 4). The largest group contributions to the binding free energy change are van der Waals contributions from Leu^{117} and Leu^{131} (−0.3 kcal/mol each, favoring 6-demethyl-Tc). The Val^{113} and Ile^{134} components are zero. In TetR(B), Leu^{117} and Leu^{131} are conserved, but Ile^{134} is replaced by a leucine, whereas Val^{113} is replaced by a leucine. Changing Val^{113} to Leu introduces an additional CH_2, which is expected to contribute ~−0.2 kcal/mol in additional van der Waals interaction energy (assuming a 4 Å distance between the Tc 6-methyl and the new CH_2). This is partly offset by CH_2-solvent interactions in the unbound state. Additional effects such as improved packing of the 6-methyl neighbors in TetR(B) (or inferior packing around the 6-demethyl variants) must account for the rest of the 1 kcal/mol binding free energy gain. To determine the precise origin would require extensive TetR(B) simulations. For the 11 other Tc variants (which are not 6-demethylated), the mean TetR(D)/TetR(B) difference is just +0.2 kcal/mol; this small, average increase in TetR(B) binding may be due to statistical noise.

Methylation or chlorination at positions 7 or 8 all have a similar effect, increasing TetR(D) binding by 0.8 kcal/mol, very similar to 6-methylation. The 8-methyl and 8-chloro groups make favorable contacts with the side chains of Leu^{131}, $Met^{177'}$, $Leu^{174'}$, $Leu^{170'}$, and $Val^{173'}$; primed residues belong to monomer 2 (Fig. 4). Interestingly, the favorable effect of 8-Cl is enhanced when an amino group is introduced at the adjacent position 9. Thus, 9-amino-8-Cl-6-deoxy-6-demethyl-Tc binds 1.1 kcal/mol more strongly than 9-amino-6-deoxy-6-demethyl-Tc. This represents a 0.3 kcal/mol enhancement for 8-chlorination when the 9-amino group is present. The enhancement is a solvent effect, arising from the ΔG_{solv} free energy terms, since the ΔG_{prot} values for 8-chlorination are the same with or without the 9-amino group (0.9 kcal/mol; Table 1). It corresponds to a partial desolvation by 8-Cl of the polar, 9-amino group: when 8-Cl is present, the 9-amino:solvent interactions in the unbound state are reduced and it is easier to desolvate the ligand.

Tc's 4-dimethylamino group contributes strongly to TetR binding

The largest binding changes are due to variations at position 4, involving the 4-dimethylamino group. Switching C4 to the epimeric configuration results in a drastic decrease of Tc binding. The experimental binding free energy increase for TetR(B) is 3.4 ± 0.4 kcal/mol; the computed value for TetR(D) is 2.8 ± 0.4 kcal/mol. Two hydrogen bonds between 4-epi-Tc and Asn^{82} are formed in the MD structure, similar to the Tc case. In the TetR(D):Tc complex, His^{64} interacts with both the O_3 and O_2' oxygens of Tc; in the 4-epi-Tc complex, the O_3-His^{64} interaction is maintained, but the O_2'-His^{64} distance is too long for a hydrogen bond (3.7 Å). Previous free energy simulations predicted that His^{64} spends almost half of its time in the singly-protonated state and the rest in the doubly-protonated state (29). In our simulations, we treat it as doubly-protonated, which may lead to overestimated interactions. The agreement with experiment suggests that the error cannot be too large; however. Both Tc and 4-epi-Tc also interact with Gln^{116}, through O_3 and O_2'. Overall, the polar interactions of Tc and 4-epi-Tc are similar, except for the lacking His^{64}-O_2' hydrogen bond with 4-epi-Tc. The steric interactions of 4-epi-Tc with TetR(D) are somewhat poorer; this is reflected by the van der Waals component of the Tc/4-epi-Tc binding free energy difference: 3.2 kcal/mol, out of the 2.8 kcal/mol total (the electrostatic component is −0.4 kcal/mol).

Removing the 4-dimethylamino group altogether reduced binding below the sensitivity of the experimental method (59). Nevertheless, the experimental binding free energy can be inferred with the help of the 4-dedimethylamino-anhydro-Tc (4-ddma-aTc) value, +2.7 ± 0.3 kcal/mol. Indeed, aTc and Tc have the same structure around positions 3–5, and the same interactions with TetR. Therefore, the binding free energy difference between Tc and 4-ddma-Tc should be close to the difference between aTc and 4-ddma-aTc, 4.8 ± 0.6 kcal/mol. The computed Tc/4-ddma-Tc difference is 4.6 ± 0.7 kcal/mol. Thus, the simulations support the idea that the 4-dimethylamino contribution is transferable between Tc and aTc, and show that TetR(B) and TetR(D) behave similarly.

Removing the 4-dimethylamino group eliminates several interactions. First, favorable van der Waals contacts are lost between the two methyls and nearby Phe^{86}, Ile^{134}, Val^{137}, and Ser^{138} (Fig. 2). Second, unfavorable methyl-water contacts in the unbound state are removed, stabilizing that state. Third, the Tc N4 makes a hydrogen bond to Asn^{82}, which is lost with 4-ddma-Tc. It is interesting to compare the effect of an Asn^{82}Ala mutation, which also eliminates this interaction, and which reduces Tc binding by 2.0 ± 1.3 kcal/mol; this last free energy change should be viewed as the difference between a strong Asn^{82}-dimethylamino interaction in the bound state and a weaker Asn^{82}-water interaction in the unbound state. Experimentally, an Asn^{82}Ser mutation reduces binding by a similar amount, 2.7 kcal/mol (63). Fourth, 4-ddma-Tc has a protonated O_3, unlike zwitterionic Tc, leading to weaker interactions with Gln^{116} and His^{64}. Mutating Gln^{116} to alanine reduces Tc

binding by 4.5 ± 0.6 kcal/mol; mutating His^{64} to Ala reduces Tc binding by 2.6 ± 0.9 kcal/mol.

DISCUSSION AND CONCLUSION

Elucidating protein-ligand binding remains an important challenge. Although experiments, especially crystallography, provide essential information, the most powerful approach, arguably, is to combine experiments with MD simulations. Indeed, with MDFE, structural and thermodynamic information are derived from the same simulations. MDFE has matured considerably, giving chemical accuracy in this study. To obtain this accuracy, two general difficulties had to be overcome. The first is force-field availability and accuracy. This is a concern whenever the ligands are not standard biopolymers and are not part of the main, existing force fields (64). Notice that general force fields are being developed and improved, such as the general AMBER force field (65) and the very recent, general CHARMM force field (66). For tetracyclines, a specific force field was developed earlier (35,36). Care was taken to maintain a good consistency and balance between the new parameters and the other, standard parts of the CHARMM force field. The second difficulty is the existence of multiple free energy minima, corresponding to different conformations and protonation states. An earlier study used special x-ray refinement methods and free energy simulations to explore Tc tautomers, His^{64} protonation states, and the orientation of important protein side chains (29). With this groundwork, MDFE gave an RMS deviation between simulations and experiments of 0.44 kcal/mol for the binding free energies of Tc and five variants. The measurements for these complexes were performed after the simulations. A similar deviation (0.35 kcal/mol) was obtained earlier for six tetracyclines binding to the 30S ribosomal particle (40). For Tc and two variants (7-chloro-Tc and 6-deoxy-5-hydroxy-Tc), the MD structures could be compared to x-ray complexes, giving good agreement. A hallmark of MDFE is that this agreement is obtained without any adjustable parameters.

The mean precision of simulations and experiment is very similar, ±0.5 kcal/mol for the binding free energies from all three datasets in Table 1: TetR(D) with MDFE or experiment, and TetR(B). The low MDFE uncertainty is obtained by running over 7 ns of dynamics for each ligand transformation. The uncertainty estimate is supported in several cases by repeated calculations that employed different pathways to transform one ligand into another. There is also an unknown, systematic error introduced by assuming His^{64} to be doubly-protonated, whereas earlier simulations predicted that it spends almost half of its time in the singly-protonated state (29). This error cannot be too large, however, since the free energies agree with experiment. In addition, the His^{64} position is in good agreement with experiment in the three cases where x-ray structures are available (see above), with RMS deviations of 0.9–1.0 Å, comparable to the protein backbone deviations.

After validation by the fluorescence titration experiments, the simulations provided new data, filling several gaps in the experimental dataset, for Tc variants that were harder to synthesize, whose fluorescence properties were unsuitable, or whose binding was too weak to be measured. Thus, TetR(D) binding free energies were obtained for 10 new tetracyclines, including three for which no TetR(B) measurement was available. One of these is 6-deoxy-6α-methyl-Tc, predicted to be the strongest binder of all, along with anhydrotetracycline, with a binding free energy 2.4 ± 0.2 kcal/mol better than Tc. Good accuracy was maintained even for the largest ligand variations (4-epi-Tc, 4-dedimethyl-Tc). Structural models were produced for all 16 complexes, only three of which have known x-ray structures. TetR(B) and TetR(D) binding were compared for 12 Tc variants, showing that for most (but not all) of the Tc substitutions, either protein can be used to understand the effect on binding. Finally, the simulations filled another gap by providing alanine-scanning mutagenesis data for a few positions around the Tc binding pocket (His^{64}, Asn^{82}, and Gln^{116}).

The main value of the simulations, however, is not to substitute for experiment, but to provide a deeper, atomistic understanding of the system. Thus, the inset in Fig. 3 shows a superposition of the 16 ligands studied here, based on their common TetR(D) partner. We see that the ligands bind to TetR in the same manner, so that ligand and protein reorganization effects largely cancel. Indeed, most of the variations in binding strength could be interpreted rather simply, either by changes in the ligand solvation in the unbound state, or by the making or breaking of protein-ligand contacts in the complex. Because the binding mode is conserved, the contacts for any of the ligands can be inferred from any of the three available protein-ligand crystal structures. This situation, with limited structural reorganization when the ligand is varied, also makes it easier to use and interpret a component analysis of the binding free energies (39). One case where the strength of the contacts is harder to infer is that of the 6-methyl group interacting with TetR(B), where small amino-acid sequence changes, relative to TetR(D), increase the ligand binding by 1 kcal/mol. In most cases, however, protein-ligand van der Waals or hydrogen-bond contacts were found to be transferable among different positions on the upper Tc edge and among different contexts. Thus, a methyl or chlorine substitution has almost the same effect at positions 6–8. Not only is the overall binding free energy preserved, but the van der Waals and electrostatic components in the protein and in the solvent as well. In a similar way, hydroxyl additions at positions 5 and 6 had the same effect in several different contexts, which could be interpreted as an increased desolvation penalty.

Evidently, effects such as these can be described with much more confidence with not only experiments but also MDFE structures and free energies in hand. This analysis illustrates the increasing potential of the method, and should aid efforts to design further variants of Tc and of the Tet Repressor.

REFERENCES

1. Chopra, I., and M. Roberts. 2001. Tetracycline antibiotics: mode of action, applications, molecular biology, and epidemiology of bacterial resistance. *Microbiol. Mol. Biol. Rev.* 65:232–260.
2. Chopra, I. 2002. New developments in tetracycline antibiotics: glycylcyclines and tetracycline efflux pump inhibitors. *Drug Resist. Updat.* 5:119–125.
3. Olson, M. W., A. Ruzin, E. Feyfant, T. S. Rush, J. O'Connell, et al. 2006. Functional, biophysical, and structural bases for antibacterial activity of tigecycline. *Antimicrob. Agents Chemother.* 50:2156–2166.
4. Schnappinger, D., and W. Hillen. 1996. Tetracyclines: antibiotic action, uptake, and resistance mechanisms. *Arch. Microbiol.* 165:359–369.
5. Kisker, C., W. Hinrichs, K. Tovar, W. Hillen, and W. Saenger. 1995. The complex formed between tetracycline repressor and tetracycline-Mg^{2+} reveals mechanism of antibiotic resistance. *J. Mol. Biol.* 247:260–280.
6. Takahashi, M., L. Altschmied, and W. Hillen. 1986. Kinetic and equilibrium characterization of the Tet repressor-tetracycline complex by fluorescence measurements. *J. Mol. Biol.* 187:341–348.
7. Orth, P., D. Schnappinger, W. Hillen, W. Saenger, and W. Hinrichs. 2000. Structural basis of gene regulation by the tetracycline inducible Tet repressor-operator system. *Nat. Struct. Biol.* 7:215–219.
8. Saenger, W., P. Orth, C. Kisker, W. Hillen, and W. Hinrichs. 2000. The tetracycline repressor: a paradigm for a biological switch. *Angew. Chem. Int. Ed.* 39:2042–2052.
9. Baron, U., and H. Bujard. 2000. Tet repressor-based system for regulated gene expression in eukaryotic cells: principles and advances. *Methods Enzymol.* 327:401–421.
10. Fussenegger, M. 2001. The impact of mammalian gene regulation concepts on functional genomic research, metabolic engineering, and advanced gene therapies. *Biotechnol. Prog.* 17:1–51.
11. Berens, C., and W. Hillen. 2003. Gene regulation by tetracyclines: constraints of resistance regulation in bacteria shape TetR for application in eukaryotes. *Eur. J. Biochem.* 270:3109–3121.
12. Berens, C., S. Lochner, S. Lober, I. Usai, A. Schmidt, et al. 2006. Subtype selective tetracycline agonists and their application for a two-stage regulatory system. *ChemBioChem.* 7:1320–1324.
13. Scholz, O., M. Kostner, M. Reich, S. Gastiger, and W. Hillen. 2003. Teaching TetR to recognize a new inducer. *J. Mol. Biol.* 329:217–227.
14. Scholz, O., E.-M. Henssler, J. Bail, P. Schubert, J. Bogdanska-Urbaniak, et al. 2004. Activity reversal of Tet repressor caused by single amino acid exchanges. *Mol. Microbiol.* 53:777–789.
15. Kamionka, A., J. O. Bogdanska-Urbaniak, O. Scholtz, and W. Hillen. 2004. Two mutations in the tetracycline repressor change the inducer anhydrotetracycline to a co-repressor. *Nucleic Acids Res.* 32:842–847.
16. Luckner, S. R., M. Klotzsche, C. Berens, W. Hillen, and Y. A. Muller. 2007. How an agonist peptide mimics the antibiotic tetracycline to induce Tet-repressor. *J. Mol. Biol.* 368:780–790.
17. Klotzsche, M., D. Goeke, C. Berens, W. Hillen, and Y. A. Muller. 2007. Efficient and exclusive induction of Tet repressor by the oligopeptide Tip results from co-variation of their interaction site. *Nucleic Acids Res.* 35:3945–3952.
18. Kamionka, A., M. Majewski, K. Roth, R. Bertram, C. Kraft, et al. 2006. Induction of single chain tetracycline repressor requires the binding of two inducers. *Nucleic Acids Res.* 34:3834–3841.
19. Hinrichs, W., C. Kisker, M. Duvel, A. Muller, K. Tovar, et al. 1994. Structure of the Tet repressor-tetracycline complex and regulation of antibiotic resistance. *Science.* 264:418–420.
20. Kedracka-Krok, S., and Z. Wasylewski. 2003. A differential scanning calorimetry study of tetracycline repressor. *Eur. J. Biochem.* 270:4564–4573.
21. Kedracka-Krok, S., A. Gorecki, P. Bonarek, and Z. Wasylewski. 2005. Kinetic and thermodynamic studies of Tet repressor-tetracycline interaction. *Biochemistry.* 44:1037–1046.
22. Henssler, E. M., R. Bertram, S. Wisshak, and W. Hillen. 2005. Tet repressor mutants with altered effector binding and allostery. *FEBS J.* 272:4487–4496.
23. Reichheld, S. E., and A. R. Davidson. 2006. Two-way interdomain signal transduction in tetracycline repressor. *J. Mol. Biol.* 361:382–389.
24. Aleksandrov, A., L. Schuldt, W. Hinrichs, and T. Simonson. 2008. Tet repressor induction by tetracycline: a molecular dynamics, continuum electrostatics, and crystallographic study. *J. Mol. Biol.* 378:896–910.
25. Orth, P., D. Schnappinger, P. Sum, G. Ellestad, W. Hillen, et al. 1999. Crystal structure of Tet repressor in complex with a novel tetracycline, 9-(*n*,*n*-dimethylglycylamido)-6-demethyl-6-deoxy-tetracycline. *J. Mol. Biol.* 285:455–461.
26. Palm, G. J., T. Lederer, P. Orth, W. Saenger, M. Takahashi, et al. 2008. Specific binding of divalent metal ions to tetracycline and to the Tet repressor/tetracycline complex. *J. Biol. Inorg. Chem.* 13:1097–1110.
27. Orth, P., F. Cordes, D. Schnappinger, W. Hillen, W. Saenger, et al. 1998. Conformational changes of the Tet repressor induced by tetracycline trapping. *J. Mol. Biol.* 279:439–447.
28. Orth, P., W. Saenger, and W. Hinrichs. 1999. Tetracycline-chelated Mg^{2+} ion initiates helix unwinding in Tet repressor induction. *Biochemistry.* 38:191–198.
29. Aleksandrov, A., J. Proft, W. Hinrichs, and T. Simonson. 2007. Protonation patterns in tetracycline-Tet repressor recognition: simulations and experiments. *ChemBioChem.* 8:675–685.
30. Tembe, B., and J. McCammon. 1984. Ligand-receptor interactions. *Comput. Chem.* 8:281–283.
31. Brooks, C., M. Karplus, and M. Pettitt. 1987. Proteins: a theoretical perspective of dynamics, structure and thermodynamics. *Adv. Chem. Phys.* 71:259–320.
32. Jorgensen, W. 1989. Free energy calculations: a breakthrough for modeling organic chemistry in solution. *Acc. Chem. Res.* 22:184–189.
33. Simonson, T., G. Archontis, and M. Karplus. 2002. Free energy simulations come of age: the protein-ligand recognition problem. *Acc. Chem. Res.* 35:430–437.
34. Chipot, C., A. E. Mark, V. S. Pande, and T. Simonson. Significant applications of free energy calculations to chemistry and biology. *In* Free Energy Calculations: Theory and Applications in Chemistry and Biology. C. Chipot and A. Pohorille, editors. Springer Verlag, New York.
35. Aleksandrov, A., and T. Simonson. 2006. The tetracycline:Mg^{2+} complex: a molecular mechanics force field. *J. Comput. Chem.* 13:1517–1533.
36. Aleksandrov, A., and T. Simonson. 2008. Molecular mechanics models for tetracycline analogues. *J. Comput. Chem.* 30:243–255.
37. Gao, J., K. Kuczera, B. Tidor, and M. Karplus. 1989. Hidden thermodynamics of mutant proteins: a molecular dynamics analysis. *Science.* 244:1069–1072.
38. Boresch, S., and M. Karplus. 1995. The meaning of component analysis: decomposition of the free energy in terms of specific interactions. *J. Mol. Biol.* 254:801–807.
39. Archontis, G., T. Simonson, and M. Karplus. 2001. Binding free energies and free energy components from molecular dynamics and Poisson-Boltzmann calculations. Application to amino acid recognition by aspartyl-tRNA synthetase. *J. Mol. Biol.* 306:307–327.
40. Aleksandrov, A., and T. Simonson. 2008. Binding of tetracyclines to elongation factor Tu, the Tet repressor, and the ribosome: a molecular dynamics simulation study. *Biochemistry.* 47:13594–13603.
41. Takahashi, M., J. Degenkolb, and W. Hillen. 1991. Determination of the equilibrium association constant between Tet repressor and tetracycline at limiting Mg^{2+} concentrations: a generally applicable method for effector-dependent high-affinity complexes. *Anal. Biochem.* 199: 197–202.
42. Beglov, D., and B. Roux. 1994. Finite representation of an infinite bulk system: solvent boundary potential for computer simulations. *J. Chem. Phys.* 100:9050–9063.

43. Simonson, T. 2000. Electrostatic free energy calculations for macromolecules: a hybrid molecular dynamics/continuum electrostatics approach. *J. Phys. Chem. B.* 104:6509–6513.

44. Mackerell, A. D., D. Bashford, M. Bellott, R. L. Dunbrack, J. Evanseck, et al. 1998. An all-atom empirical potential for molecular modeling and dynamics study of proteins. *J. Phys. Chem. B.* 102:3586–3616.

45. Jorgensen, W., J. Chandrasekar, J. Madura, R. Impey, and M. Klein. 1983. Comparison of simple potential functions for simulating liquid water. *J. Chem. Phys.* 79:926–935.

46. Stote, R., D. States, and M. Karplus. 1991. On the treatment of electrostatic interactions in biomolecular simulation. *J. Chim. Phys.* 88: 2419–2433.

47. Brooks, B., R. Bruccoleri, B. Olafson, D. States, S. Swaminathan, et al. 1983. CHARMM: a program for macromolecular energy, minimization, and molecular dynamics calculations. *J. Comput. Chem.* 4:187–217.

48. Brooks, B., C. L. Brooks, III, A. D. Mackerell, Jr., L. Nilsson, R. J. Petrella, et al. 2009. CHARMM: the biomolecular simulation program. *J. Comput. Chem.* 30:1545–1614.

49. Simonson, T. 2001. Free energy calculations. *In* Computational Biochemistry and Biophysics. O. Becker, A. Mackerell, Jr., B. Roux, and M. Watanabe, editors. Marcel Dekker, New York.

50. Simonson, T. 1993. Free energy of particle insertion. an exact analysis of the origin singularity for simple liquids. *Mol. Phys.* 80:441–447.

51. Hodel, A., T. Simonson, R. O. Fox, and A. T. Brünger. 1993. Conformational substates and uncertainty in macromolecular free energy calculations. *J. Phys. Chem.* 97:3409–3417.

52. Reinhardt, W., M. Miller, and L. Amon. 2001. Why is it so difficult to simulate entropies, free energies, and their differences? *Acc. Chem. Res.* 34:607–614.

53. Shirts, M. R., J. W. Pitera, W. C. Swope, and V. S. Pande. 2003. Extremely precise free energy calculations of amino acid side chain analogs: comparison of common molecular mechanics force fields for proteins. *J. Chem. Phys.* 119:5740–5761.

54. Hermans, J. 1991. Simple analysis of noise and hysteresis in (slow-growth) free energy simulations. *J. Phys. Chem.* 95:9029–9032.

55. Wood, R. H. 1991. Estimation of errors in free energy calculations due to the lag between the Hamiltonian and the system configuration. *J. Phys. Chem.* 95:4838–4842.

56. Hummer, G. 2001. Fast growth thermodynamic integration: error and efficiency analysis. *J. Chem. Phys.* 114:7330–7337.

57. Thompson, D., P. Plateau, and T. Simonson. 2006. Free energy simulations reveal long-range electrostatic interactions and substrate-assisted specificity in an aminoacyl-tRNA synthetase. *ChemBioChem.* 7: 337–344.

58. Thompson, D., and T. Simonson. 2006. Molecular dynamics simulations show that bound Mg^{2+} contributes to amino acid and aminoacyl adenylate binding specificity in aspartyl-tRNA synthetase through long-range electrostatic interactions. *J. Biol. Chem.* 281:23792–23803.

59. Lederer, T., M. Kintrup, M. Takahashi, P. E. Sum, G. A. Ellestad, et al. 1996. Tetracycline analogs affecting binding to Tn10-encoded Tet repressor trigger the same mechanism of induction. *Biochemistry.* 35:7439–7446.

60. Fersht, A. 1987. The hydrogen bond in molecular recognition. *Trends Biochem. Sci.* 12:301–304.

61. Fersht, A. 1999. Structure and Mechanism in Protein Science: a Guide to Enzyme Catalysis and Protein Folding. Freeman, New York.

62. Buck, M., and M. Karplus. 2001. Hydrogen bond energetics: a simulation and statistical analysis of *n*-methyl acetamide, water, and human lysozyme. *J. Phys. Chem. B.* 105:11000–11015.

63. Müller, G., B. Hecht, V. Helbl, W. Hinrichs, W. Saenger, et al. 1995. Characterization of non-inducible Tet repressor mutants suggests conformational changes necessary for induction. *Nat. Struct. Biol.* 2:693–703.

64. Jorgensen, W. L., and J. Tirado-Rives. 2005. Potential energy functions for atomic-level simulations of water and organic and biomolecular systems. *Proc. Natl. Acad. Sci. USA.* 102:6665–6670.

65. Wang, J., R. M. Wolf, J. W. Caldwell, P. A. Kollman, and D. A. Case. 2004. Development and testing of a general AMBER force field. *J. Comput. Chem.* 25:1157–1174.

66. Vanommeslaeghe, K., E. Hatcher, C. Acharya, S. Kundu, S. Zhong, et al. 2009. CHARMM general force field: a force field for drug-like molecules compatible with the CHARMM all-atom additive biological force fields. *J. Comp. Chem.* In press.